SANDIA REPORT

SAND2005-7557
Unlimited Release
Printed November 2005

Development and Integration of Raman Imaging Capabilities to Sandia National Laboratories Hyperspectral Fluorescence Imaging Instrument

Jerilyn A. Timlin, Linda T. Nieman

Prepared by
Sandia National Laboratories
Albuquerque, New Mexico 87185 and Livermore, California 94550

Sandia is a multiprogram laboratory operated by Sandia Corporation,
a Lockheed Martin Company, for the United States Department of Energy's
National Nuclear Security Administration under Contract DE-AC04-94AL85000.

Issued by Sandia National Laboratories, operated for the United States Department of Energy by Sandia Corporation.

Available to DOE and DOE contractors from
U.S. Department of Energy
Office of Scientific and Technical Information
P.O. Box 62
Oak Ridge, TN 37831

Telephone: (865)576-8401
Facsimile: (865)576-5728
E-Mail: reports@adonis.osti.gov
Online ordering: http://www.osti.gov/bridge

Available to the public from
U.S. Department of Commerce
National Technical Information Service
5285 Port Royal Rd
Springfield, VA 22161

Telephone: (800)553-6847
Facsimile: (703)605-6900
E-Mail: orders@ntis.fedworld.gov
Online order: http://www.ntis.gov/help/ordermethods.asp?loc=7-4-0#online

SAND 2005-7557
Unlimited Release
Printed November 2005

Development and Integration of Raman Imaging Capabilities to Sandia National Laboratories Hyperspectral Fluorescence Imaging Instrument

Jerilyn A. Timlin and Linda T. Nieman

Biomolecular Imaging and Analysis
Sandia National Laboratories
PO Box 5800
Albuquerque, NM 87185-0895

Abstract

Raman spectroscopic imaging is a powerful technique for visualizing chemical differences within a variety of samples based on the interaction of a substance's molecular vibrations with laser light. While Raman imaging can provide a unique view of samples such as residual stress within silicon devices, chemical degradation, material aging, and sample heterogeneity, the Raman scattering process is often weak and thus requires very sensitive collection optics and detectors. Many commercial instruments (including ones owned here at Sandia National Laboratories) generate Raman images by raster scanning a point focused laser beam across a sample – a process which can expose a sample to extreme levels of laser light and requires lengthy acquisition times. Our previous research efforts have led to the development of a state-of-the-art two-dimensional hyperspectral imager for fluorescence imaging applications such as microarray scanning. This report details the design, integration, and characterization of a line-scan Raman imaging module added to this efficient hyperspectral fluorescence microscope. The original hyperspectral fluorescence instrument serves as the framework for excitation and sample manipulation for the Raman imaging system, while a more appropriate axial transmissive Raman imaging spectrometer and detector are utilized for collection of the Raman scatter. The result is a unique and flexible dual-modality fluorescence and Raman imaging system capable of high-speed imaging at high spatial and spectral resolutions. Care was taken throughout the design and integration process not to hinder any of the fluorescence imaging capabilities. For example, an operator can switch between the fluorescence and Raman modalities without need for extensive optical realignment. The instrument performance has been characterized and sample data is presented.

Acknowledgements

The authors wish to thank Michael B. Sinclair for design and construction of the original hyperspectral fluorescence imaging system and sharing his optical design expertise and knowledge of the existing hyperspectral fluorescence imaging system to allow us to better integrate the two imaging modalities. The authors also thank Christopher A. Gresham and Jaime Reif for allowing us to conduct initial experiments on their Nicolet Almega Raman microprobe instrument and for their invaluable assistance in performing these experiments. In addition, the authors thank Carol I. Ashby for her generous donation of the Princeton Instruments charge-coupled-device detector utilized in the results presented in this report.

Table of Contents

Acknowledgements **4**
Nomenclature **6**
Design considerations **8**
Final design and construction **8**
Raman imaging module characterization **11**
Conclusions **16**
References **17**
Distribution **18**

List of Figures

Figure 1: Hyperspectral imaging system layout (fluorescence) 7
Figure 2: Hyperspectral imaging system layout (Raman) 8
Figure 3: Typical spectral calibration 9
Figure 4: Raman spectrum of Teflon® tape taken with a 50 μm slit 10
Figure 5: Resolution target images illustrating imaging capability and spatial resolution of Raman module 121
Figure 6: Hyperspectral Raman image of a silicon wafer and Teflon® sample 122

List of Tables

Table 1: Spectral characteristics of Raman module 12
Table 2: Major Raman Lines of Teflon® from Literature 12

Nomenclature

2D	Two-dimensional
BS	Beamsplitter
CCD	Charge coupled device
HSI	Hyperspectral imaging
HS	Hyperspectral
LN	Liquid nitrogen

Introduction

Raman spectroscopic imaging is a non-destructive surface technique with excellent selectivity and sensitivity for organic and inorganic material characterization by probing the vibrational structure of the material with the spatial resolution of a light microscope.(Batchelder et al., 1991; Schrader, 1995) Raman spectroscopy is often a more desirable platform for microscopic imaging of defects and substructures than its much utilized complimentary spectroscopic imaging counterpart, infrared imaging, due to its increased spatial resolution, ease of sample preparation, and lack of interference from water and water vapor. Raman spectroscopic imaging can offer a unique tool for visualizing chemical structure non-destructively within intact systems and components and has the potential to identify irregularities in the chemical composition of the material and/or coatings. These abilities could impact a variety of Sandia National Laboratories communities concerned with the characterization and reliability of microsystems such as Micro-Electro-Mechanical Systems (MEMS), non-nuclear stockpile components, microfluidic devices, and thin film structures and is important for early detection and mapping of age-based degradation. In addition, potential applications exist in Sandia's biological research communities.

Although Raman spectroscopy and some basic Raman microsampling capabilities exist at Sandia at the writing of this report there are no systems capable of true Raman spectral imaging. While Raman microsampling microscopes (also known as Raman microprobes or point-mapping systems) can be very useful for some applications they are often limited in terms of image acquisition and mapping times because they operate as point or raster scanning devices. This is especially true when considering the longer integration times typically used for Raman spectroscopy (minutes to tens of minutes). Raman imaging methodologies have been compared elsewhere.(Schlucker et al., 2003) Commercial Raman imaging systems are available based on line-imaging, point-scanning or global illumination, but are cost prohibitive with the funding available at the time of this project and possess software overhead that does not allow the full imaging speed potential to be realized.

Recent projects in our laboratory have led to the construction of a hyperspectral line-scan imaging system capable of rapidly collecting an entire fluorescence emission spectrum at each image pixel.(Sinclair et al., 2004) the line-scan or push-broom architecture of our fluorescence system provides a nice compromise between a point or raster scanned microscope and a global illumination based imaging microscope. While our instrument implements the fastest read-out speed available for its hardware, the spectrometer on the existing system was chosen based on its spectral coverage, spectral resolution, and sensitivity necessary for fluorescence spectroscopy and thus is not appropriate for Raman spectroscopic imaging, though all the rest of the optics are. A simple switch of spectrometers is not a viable option as the fundamental differences between these two spectroscopies make it difficult to satisfy the requirements of both simultaneously. In this report we present the design and subsequent characterization of a Raman imaging module that was constructed and integrated into the existing fluorescence hyperspectral imager. This module provides Raman imaging capabilities at Sandia in a unique dual-modality system. By coupling to our existing equipment for the laser illumination and high-speed, high accuracy motion control portions of the instrument we have leveraged our past research as much as possible.

Design considerations

Three main categories of requirements drove the design process – impact on existing imager and projects, ease of switching between imaging configurations, and Raman specific spectral resolution and spectral range requirements. In addition, though there was no outright requirement, attempts were made to facilitate dual-modality imaging with this integrated system. (Dual-modality imaging is defined as the ability to image the same area on a sample in one modality and then the other simultaneously or serially.)

At the time the design began there were at least 6 funded projects and 3 researchers utilizing the hyperspectral fluorescence imager and it was critical that the integration of the Raman imaging module have as little negative impact as possible on these existing projects. Three major upgrades to the existing imager were planned – a complete overhaul of the objective and beamsplitter mounting hardware to provide additional flexibility and usability, a switch to improved motion controllers, and a replacement of the existing spectrometer and detector with a custom design prism spectrometer and higher speed detector capable of improved sensitivity and speed. Deadlines and time constraints on these projects affected the ability to begin and finish these upgrades as well as the integration of the Raman module. At present only the first two upgrades have been completed. They were accomplished before the integration of the Raman system and they provided improvements to the instrument performance necessary to perform both the fluorescence and Raman imaging functions.

One of the challenges of any multiple use platform is ease of switching between configurations. If it is too cumbersome for a user to switch between excitation laser or fluorescence and Raman spectrometers then time is not being used effectively and projects on both systems suffer. When this project began there were two lasers available for the hyperspectral fluorescence imaging system and it would take approximately ½ to one full day to rearrange the optics to change excitation lasers. This was unacceptable and the project leads agreed that ideal times to alter configurations should be on the order of minutes, not hours and should possess the potential to be automated. These requirements are achievable through the use of high precision flip-in type mirrors and kinematic mounts.

Raman spectroscopy itself brought some specific design requirements into consideration when choosing the spectrometer to purchase for the Raman module. The spectrometer needed to posses high sensitivity, high spectral resolution, flexibility to allow us to utilize several lasers for excitation, and an f-number that would maximize compatibility with our existing optical train. Spectral coverage and range was not critical since Raman spectroscopy in the fingerprint regime only needs to extend ~100 nm from the excitation laser line.

Final design and construction

Figure 1 shows the two-dimensional hyperspectral instrument layout with the green laser (25 mW single mode 532 nm, Crystal Laser GCL-025s) excitation fluorescence configuration. The green laser excitation path is highlighted in green and fluorescence collection path is highlighted in orange. The details of this portion of the optical layout are documented elsewhere.(Sinclair et al., 2004) Two modifications to the system outlined in the previously published literature include the microscope objective

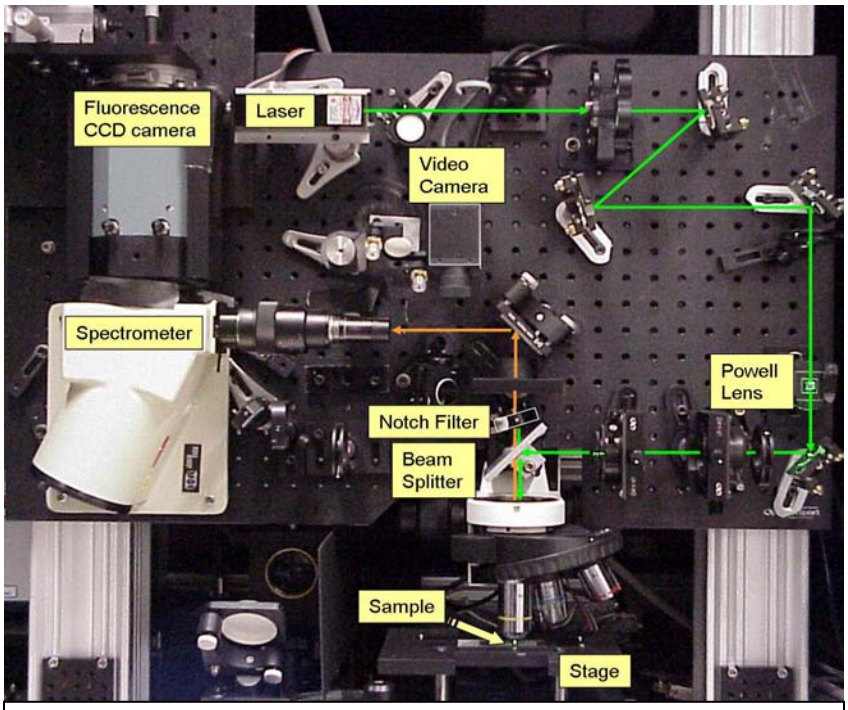

Figure 1: Hyperspectral imaging system layout shown with green laser excitation fluorescence configuration. Green lines indicate the laser optical path. Orange lines indicate collected fluorescence from sample. The notch filter rejects any remaining laser light.

nose piece that allows for easy switching between microscope objectives (Nikon Optical Components, BD series 5pl nosepiece) and the beamsplitter (BS)/notch filter mounting hardware. The BS and notch filter in this arrangement are mounted on a kinematic base (Newport Corporation BK-2A) that allow for the entire unit to be removed and replaced with high repeatability with one of the following options – 1) a different BS and notch filter combination to accommodate additional excitation lasers for fluorescence imaging or, 2) a BS and mirror configuration to direct the beam to the Raman imaging module. Figure 2 shows the hyperspectral imaging system with the red laser excitation Raman configuration. The red laser (25 mW 638 nm diode laser, Crystal Laser RCL-025m) excitation path is highlighted in red and the Raman scatter collection path is highlighted in purple. The beamsplitters employed for either red excitation (Chroma Technology Corporation, Z633 RDC) or green excitation (Chroma Technology Corporation, Z532 RDC) are suitable for Raman or fluorescence applications. The hardware can be easily configured by swapping the necessary pre-aligned kinematic base mounts to allow hyperspectral Raman or fluorescence imaging with excitation by either laser without need for extensive realignment.

Following the BS, the collected, collimated Raman scatter is projected through series of three high quality mirrors (Newport Corporation, 20D20BD.1, 1/10 wave or 10D20BD.1, 1/10 wave) and a holographic notch filter (Kaiser Optical Systems, Inc. HNPF633 or HNPF532) to transport the light from the breadboard to the optics mounted on the optical table and reject scattered laser light. Once at the optical table a lens (Melles Griot, 300 mm achromat) focuses the beam onto the entrance slit of the axial transmissive spectrometer (Kaiser Optical Systems, Inc., Holospec 1.8i NIR optimized). The spectrometer design provides excellent spectral resolution and alignment stability.(Owen

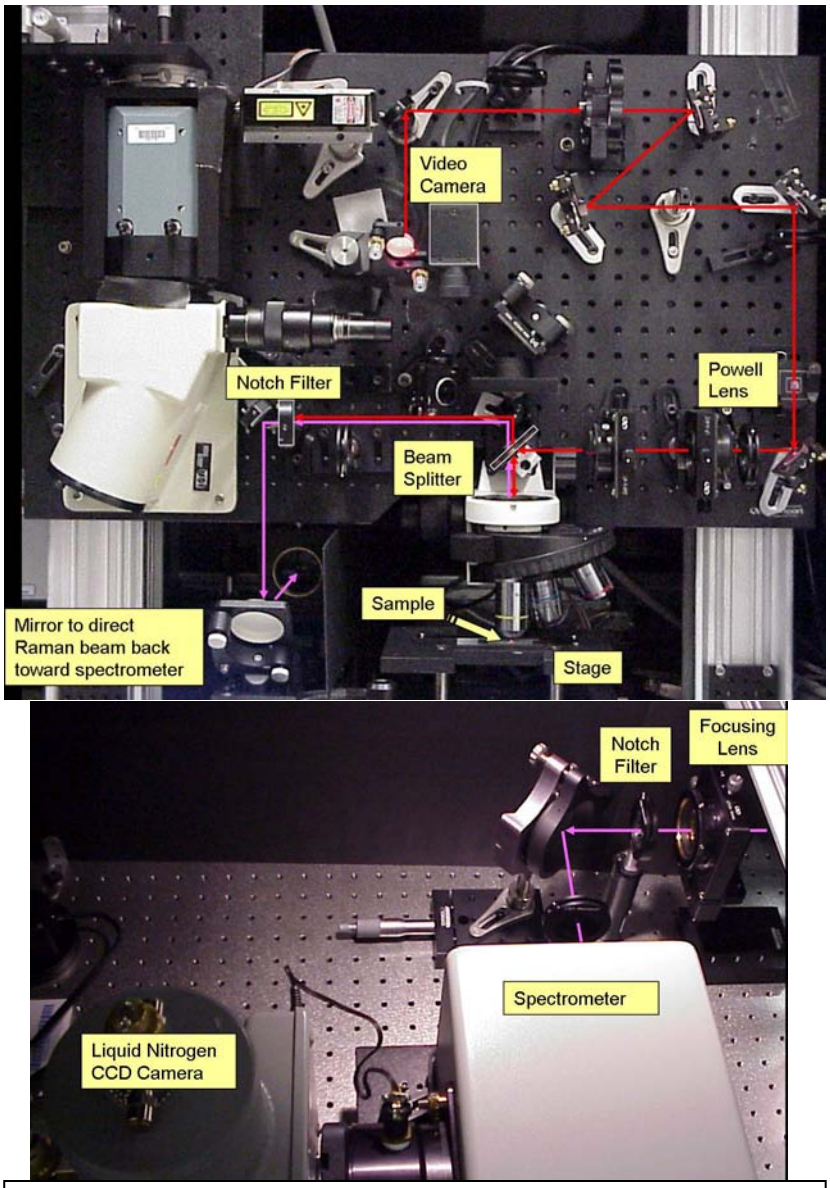

Figure 2: Hyperspectral imaging system layout shown with red laser excitation Raman configuration. Red lines indicate the laser optical path. Purple lines indicate collected Raman scatter. Top Panel: Front view of instrument. Bottom panel: Side view of Raman module showing focusing lens, notch filter, mirror, spectrometer and detector.

et al., 1995) Several gratings have been purchased for the spectrometer (Kaiser Optical Systems, Inc.) allowing Raman imaging with green or red excitation. Currently a liquid nitrogen (LN) charge-coupled device (CCD) detector is connected to the spectrometer (Princeton Instruments, LNCCD1152). Although the EM-CCD used in the fluorescence system is faster, more sensitive, and more modern, it is an imaging detector and thus does not have enough pixels in the spectral dimension to permit a full Raman fingerprint spectrum to be acquired and thus it was not utilized in these initial characterization studies.

Generation of a Raman hyperspectral image requires that the stage movement and the LN CCD readout be synchronized. In contrast to the fluorescence system stage setup, where the stage moves continuously while the camera reads out, the Raman stage movement must be incremental to accommodate the inherent slow readout rates of the LN CCD.

Synchronization of the stage and LN CCD is controlled through the commercial Aerotech stage software. A script was written in which the user assigns the stage step size, the total number of steps, and the time between each step. The step size is set to 0.01 mm for the 10x objective and 0.001 mm for the 60x objective. Each discrete step is

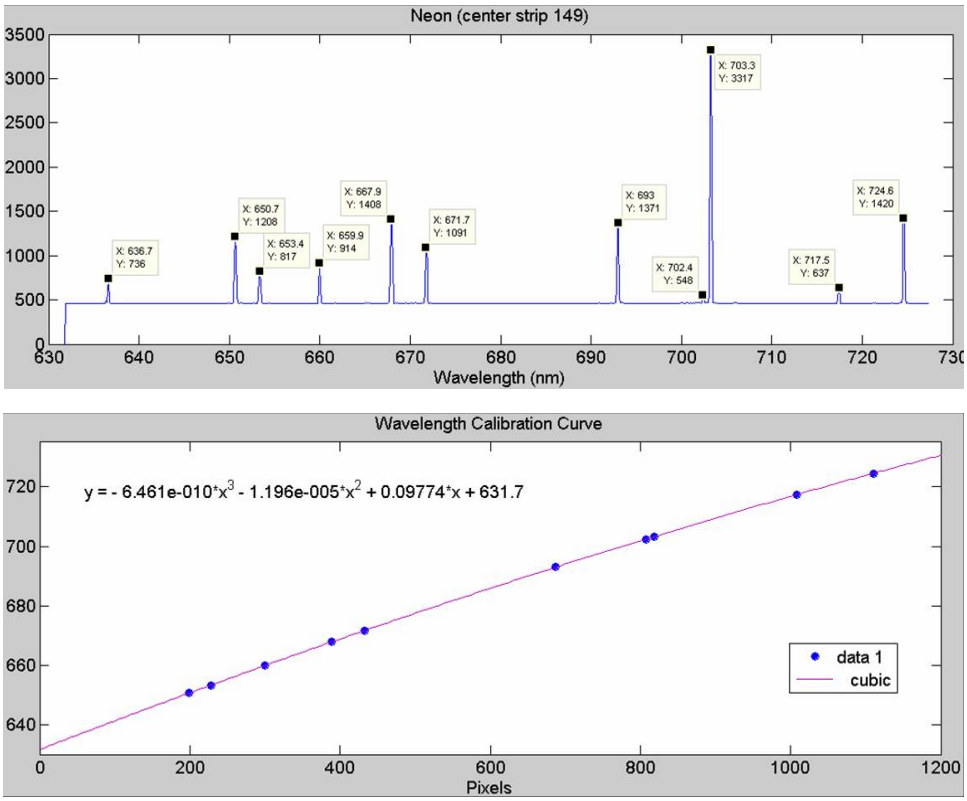

Figure 3: Typical spectral calibration using a neon pen light source and 633 nm low frequency Raman grating.

followed by a defined dwell or waiting period to allow sufficient time for the LN CCD to read out a full frame.

At the direction of the user, a 10 ms TTL (transistor-transistor logic) low pulse is generated by the stage software and sent to the LN CCD which initiates the LN CCD to read out. This cycle is repeated until the stage has traveled the prescribed distance. During image acquisition, the trigger pulses and the LN CCD readout is monitored using an oscilloscope.

Raman imaging module characterization

Characterization of the Raman imaging module was carried out primarily using the red laser excitation configuration. Wavelength calibration was performed by fitting the emission peak positions from a neon spectral pen lamp (Spectra Physics, Inc.) to a cubic equation. A typical wavelength calibration for the 633 nm low frequency Raman holographic grating (Kaiser optical Systems, Inc., HSG-632.8-LF) is shown in Figure 3. Table 1 gives values for the spectral characteristics of the Raman module. These values were determined from a cubic fit of the neon emission spectrum with the spectrometer equipped with the 633 nm low frequency Raman grating. All numbers are in direct concordance with theoretical calculations and manufacturer's specifications. Teflon® is often used as a Raman standard because of its easily identifiable Raman spectrum. Figure 4 shows the spectrum

Table 1
Spectral characteristics of Raman module determined using 633 nm low frequency grating.

	Nanometers (nm)	Relative Wavenumbers (cm^{-1})
Spectral range	631.8 – 727.4 (cubic)	-121.9 – 1959.1 (cubic)
Spectral resolution	0.12 (25 micron slit) 0.16 (50 micron slit)	2.6 (25 micron slit) 3.5 (50 micron slit)
Laser line	636.7 (cubic)	0 (by definition)

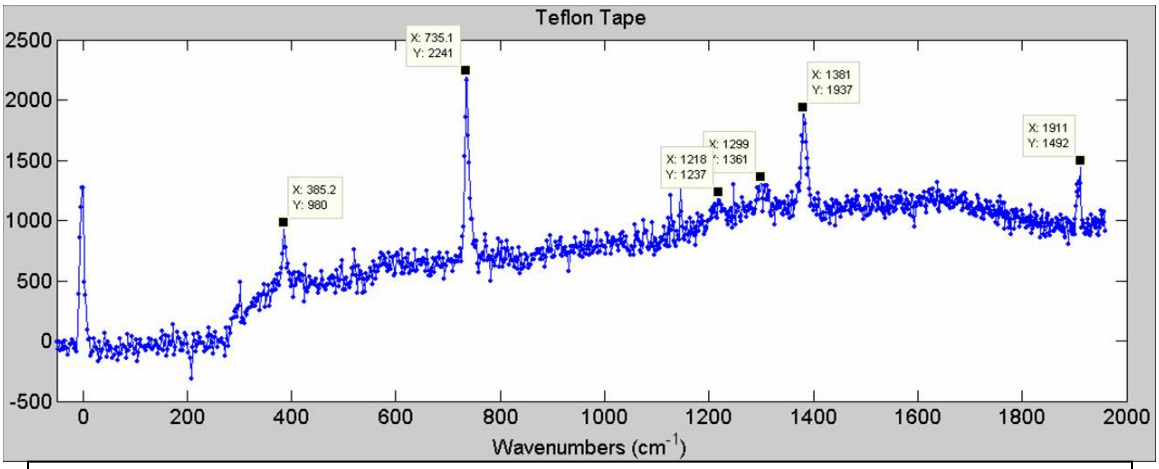

Figure 4 Raman spectrum of Teflon® tape taken with a 50 μm slit. Major peaks measured correspond with literature values (see Table 2) within the spectral resolution of Raman module.

of Teflon® tape (typically used for plumbing applications). All peak positions matched well with literature values shown in Table 2.(Lin-Vien et al., 1991) The weak fluorescent background is most likely due to other constituents in the Teflon® tape sample.

The spatial resolution (or 2 times the image pixel size as defined by the Nyquist criteria) of the Raman system will vary with objective used and can be asymmetric in a line imaging instrument, i.e. the spatial resolution in the X is different from the spatial resolution in the Y. This is possible because the spatial resolution in the X is controlled by the step size and resolution of the positioners (Aerotech) and the spatial resolution in the Y dimension is controlled by the magnification of the image and the CCD pixel size. Using a USAF 1951 resolution target (Newport Corporation) the pixel dimensions in the Y

Table 2
Major Raman Lines of Teflon® from Literature

Position (cm^{-1})	Relative Strength
385	13
732	46
1215	4
1297	7.5
1379	23

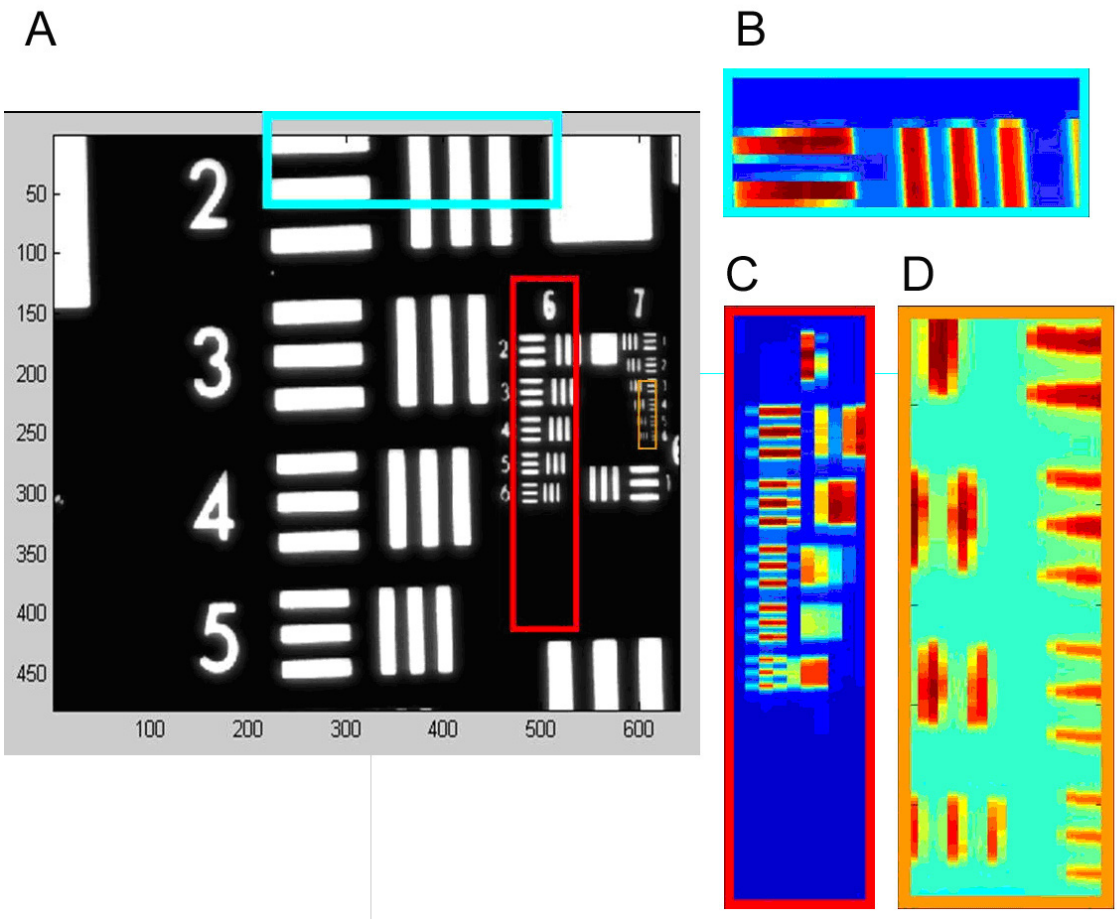

Figure 5: Resolution target images illustrating imaging capability and spatial resolution of Raman module. A. Video image of USAF 1951 resolution target. Areas of the bar target imaged with the Raman module are shown outlined with colored rectangles and used to determine lateral resolution along the direction of the spectrometer slit. B- C. Raman images taken with a 10x objective of areas outlined in cyan and red rectangles in A. D. Raman images taken with the 60x objective of the finest bar target spacing, shown in the orange rectangle in A.

(vertical, spectrometer slit) dimension with a 10x objective (NA= 0.45, CFI Plan Apochromat, Nikon USA.) to be 1.32 um/pixel. Using a 60x dry objective (NA = 0.95 CFI Plan Apochromat, Nikon USA) the vertical image pixels were 0.23 microns. This indicates near-diffraction limited imaging performance for this objective and arrangement. Previous experiments with the fluorescence imager determined that the positioners have far superior resolution than necessary for optical imaging, the positioner motion can be adjusted to make the X image pixels (generated by the stage motion in the X direction on a sample) and Y image pixels (generated by the spectrometer vertical pixels on the CCD camera and magnification along the slit dimension) equal if desired. Resolution target images used to determine the image pixel size in the Y dimensions for the 10x and 60x objective arrangement are shown in Figure 5.

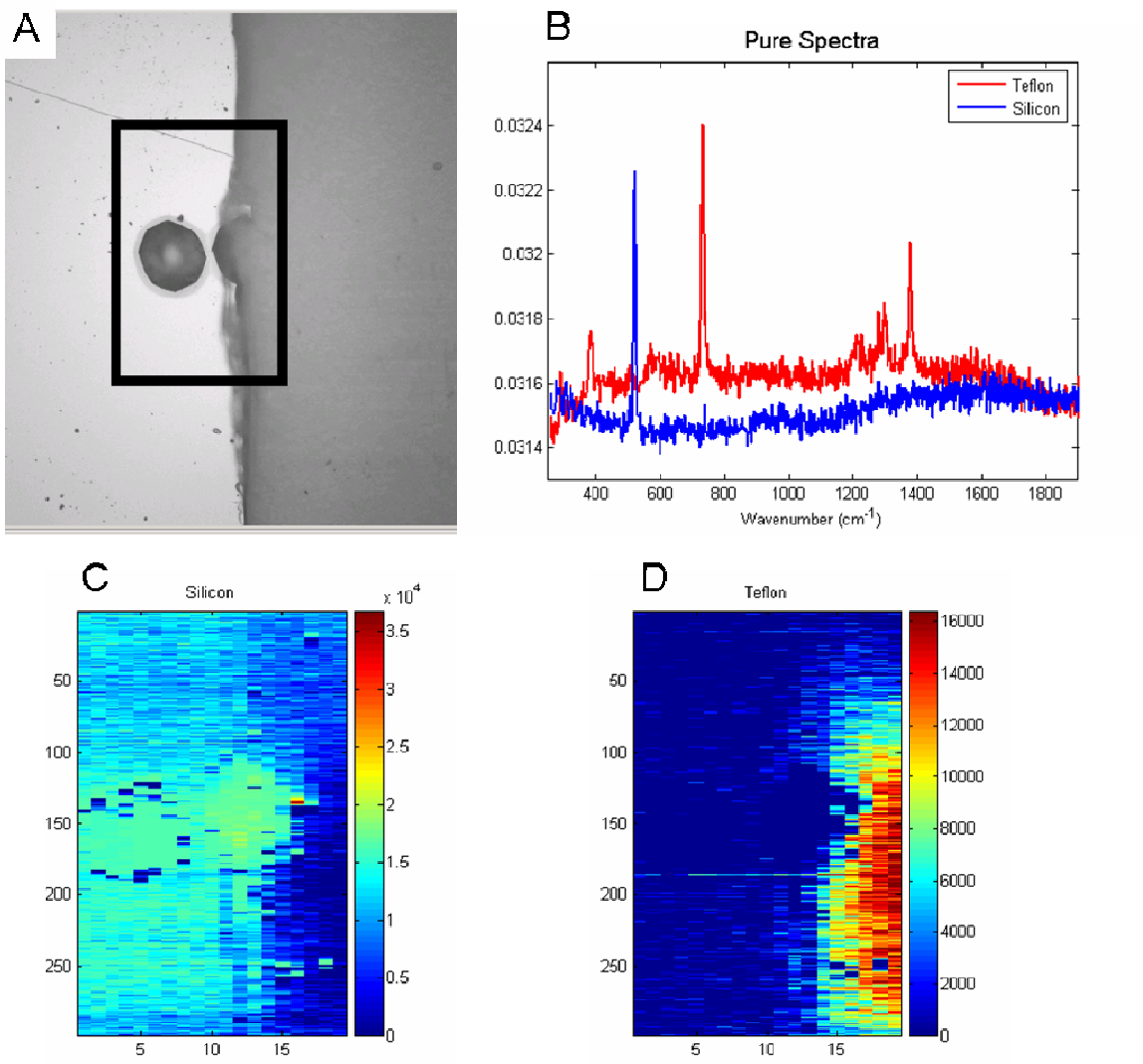

Figure 6: Hyperspectral image of a silicon wafer adjacent to Teflon® tape. A. Video image of sample. The left portion of the image consists of a fractured silicon wafer that includes a circular indentation from a portion of a serial number imprint. The dark region to the right is Teflon® tape. The imaging region is indicated by the black rectangle. B. Component emission spectra obtained from sample. C-D. Hyperspectral Raman images of silicon (C) and Teflon® (D). Bright areas in silicon and Teflon® images correspond to their locations in video image.

Using the 638 nm red laser excitation and the Princeton Instruments LN-cooled CCD arrangement characterized above, a Raman image of a test specimen comprised of Teflon® tape adjacent to a fractured silicon wafer was taken using the 10x objective to demonstrate the imaging capabilities with a multi-component sample. A bright field image of the sample is shown in Figure 6a. The area imaged by the hyperspectral system is shown by a black rectangle. The resulting component Raman spectra are shown in Figure 6b. The relative strengths and locations of the Raman peaks are consistent with literature values.(Lin-Vien et al., 1991) Concentration maps of the silicon and Teflon®

are shown in Figure 6c&d, respectively. The silicon and Teflon® images regions are easily identified in the hyperspectral images and correspond with the video image of the sample. The outer portion of the circular indentation is prominent in the silicon concentration image. This can be attributed to the spectral shift that occurs in stressed silicon.

While the image quality was excellent indicating the success of the optical integration, the logistics of using the detector was suboptimum at best. Due to the age of the detector and its controller (purchased in 1992) it was necessary to use a computer with an older style motherboard architecture and a DOS based operating system to communicate with the detector. This coupled with our internal computer security requirements for legacy machines not to be connected to the network prohibited the collection of larger Raman image data sets that could not be transferred on handful of 3 ½ inch floppy disks. Although the detector itself is in very good condition and appropriate for the imaging technique at hand, we discovered that the manufacturer no longer supports that model and thus the cost to upgrade the controller and computer interface to a Windows-based system would almost equal the cost of a new CCD detector. Considering the age of the detector this was an unattractive option.

Conclusions

The current hyperspectral imaging capabilities at Sandia National Laboratories have been expanded to include high fidelity Raman imaging. This was accomplished via the addition of a Raman module consisting of the necessary transfer optics, spectrometer, and detector to the existing 2D hyperspectral fluorescence imaging system without sacrificing any of the fluorescence imaging instrument's capabilities. In this report we have demonstrated successful integration and excellent spatial and spectral resolution performance of the Raman module. When and if a new modern detector is purchased for this instrument, Sandia researchers have available to them a unique and extremely flexible dual modality instrument providing easy access to both Raman and fluorescence images of the same area of a sample that will facilitate new areas of research on complex systems in materials and biology.

References

Batchelder, D. N., Cheng, C., and Pitt, G. D. (1991). Molecular imaging by Raman microscopy. *Advanced Materials* 3, 566-568.

Lin-Vien, D., Colthup, N. B., Fateley, W. G., and Grasselli, J. G. (1991). "The handbook of infrared and Raman characteristic frequencies of organic molecules." Academic Press, San Diego.

Owen, H., Battey, D. E., Pelletier, M. J., and Slater, J. B. (1995). New spectroscopic instrument based on volume holographic optical elements. *Proceedings of the Society of Photo-Optical Instrumentation Engineers* 2406, 260-267.

Schlucker, S., Schaeberle, M. D., Huffman, S. W., and Levin, I. W. (2003). Raman microspectroscopy: A comparison of point, line, and wide-field imaging methodologies. *Analytical Chemistry* 75, 4312-4318.

Schrader, B. (1995). "Infrared and Raman spectroscopy." VCH Publishers, Inc., New York.

Sinclair, M. B., Timlin, J. A., Haaland, D. M., and Werner-Washburne, M. (2004). Design, construction, characterization, and application of a hyperspectral microarray scanner. *Applied Optics* 43, 2079-2089.

Distribution

External:
Steve Modiano
Monsanto Corporation
800 North Lindbergh Blvd.
Mail Stop S3C
St Louis, MO 63167

Internal:

1	MS 0885	Richard Salzbrenner
8	MS 0895	Jerilyn Timlin
1	MS 0895	Anthony Martino
1	MS 0895	David Haaland
1	MS 0895	Howland Jones
1	MS 1411	Michael Sinclair
1	MS 1413	Linda Nieman
1	MS 1455	Christopher Gresham
2	MS 9018	Central Technical Files, 8945-1
2	0899	Technical Library, 4536